A new way to search for right-handed currents in semileptonic $B \to \rho \ell \bar{\nu}$ decay

Florian U. Bernlochner[a,b], Zoltan Ligeti[c], Sascha Turczyk[d]

[a]*University of Victoria, Victoria, British Columbia, Canada V8W 3P*
[b]*Physikalisches Institut der Rheinische Friedrich-Wilhelms-Universität Bonn, 53115 Bonn, Germany*
[c]*Ernest Orlando Lawrence Berkeley National Laboratory, University of California, Berkeley, CA 94720*
[d]*PRISMA Cluster of Excellence & Mainz Institut for Theoretical Physics, Johannes Gutenberg University, 55099 Mainz, Germany*

Abstract

There exist a long standing tension among determinations of the CKM matrix element $|V_{ub}|$ from various (semi)leptonic B decay channels with varying significance of up to $\sim 3\sigma$. An interesting possibility to ease this tension is to allow for a right-handed contribution to the standard model left-handed weak current mediating the $b \to u$ quark decay. Current bounds on such a contribution are fairly weak. We propose a new way to search for such a right-handed current in semileptonic $B \to \rho$ meson decays. We describe a new variable that we propose, and discuss the theoretical uncertainties. Especially we investigate the uncertainties and their correlations among all contributing form factors with the assumed z-expansion for its shape, valid over the whole q^2 range. Then we study the achievable sensitivity both from the available Babar and Belle data sets, as well as from an anticipated $50 \, \text{ab}^{-1}$ at Belle II.

1. Introduction

In the determination of the Cabbibo-Kobayashi-Maskawa (CKM) matrix element $|V_{ub}|$ a tension of almost 3σ persists between the extraction using leptonic, inclusive and exclusive semileptonic decay channels already for a long time. A precise determination of this quantity is crucial for testing the unitarity properties of the CKM matrix and also for improving tests of the Standard Model (SM), in particular to increase sensitivity to New Physics (NP) in $B^0 - \bar{B}^0$ mixing [1].

It is possible that this tension is related to not sufficiently understood theoretical or experimental details, and the larger dataset of Belle II may resolve this issue. Another possibility which would ease this tension, is to allow for a right-handed current [2, 3, 4]. For the purpose of testing this Ansatz, we consider the effective Lagrangian with only one new parameter ϵ_R,

$$\mathcal{L}_{\text{eff}} = -\frac{4G_F}{\sqrt{2}} V_{ub}^L (\bar{u}\gamma_\mu P_L b + \epsilon_R \, \bar{u}\gamma_\mu P_R b)(\bar{\nu}\gamma^\mu P_L \ell) + \text{h.c.}, \quad (1)$$

Decay	$|V_{ub}| \times 10^3$	ϵ_R dependence
$B \to \pi \, \ell \bar{\nu}$	3.23 ± 0.30	$1 + \epsilon_R$
$B \to X_u \ell \bar{\nu}$	4.39 ± 0.21	$\sqrt{1 + \epsilon_R^2}$
$B \to \tau \, \bar{\nu}_\tau$	4.32 ± 0.42	$1 - \epsilon_R$
Decay	$\mathcal{B} \times 10^4$	
$B \to \rho \, \ell \bar{\nu}$	$1.97 \pm 0.16 \, (q^2 < 12 \, \text{GeV}^2)$	
$B \to \omega \, \ell \bar{\nu}$	$0.61 \pm 0.11 \, (q^2 < 12 \, \text{GeV}^2)$	

Table 1: The $|V_{ub}|$ measurements [9] used in the fit shown in Fig. 1 and their dependence on ϵ_R. The branching fractions are taken from Ref. [10]

where $P_{L,R} = (1 \mp \gamma_5)/2$. The SM is recovered as $\epsilon_R \to 0$. The current measurements of $|V_{ub}|$ are summarized in Table 1. We indicate their dependence on ϵ_R in the simple cases. In case of a final state vector meson this is not as easy, and it depends on the considered q^2 interval. In the endpoint phase-space limits $q^2 \to 0, q_{\text{max}}^2$ the axial-vector dominates and hence we would have a simple $1 - \epsilon_R$ dependence. However such an extraction, similar to $B \to D^{(*)}$ [5], is currently
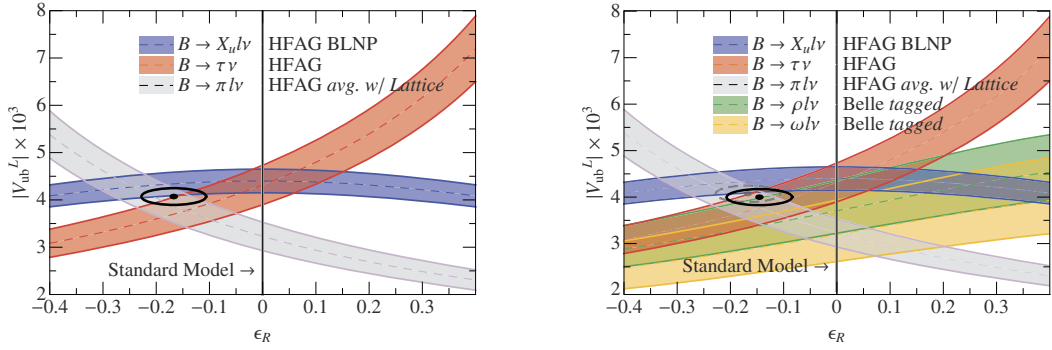
Figure 1: The allowed $|V_{ub}^L| - \epsilon_R$ regions. The black ellipse in the left (right) plot shows the result of a χ^2 fit using the first three (four, excluding ω) measurements in Table 1. The fainter ellipse in the right plot is the same as that in the left plot.

not performed, because only a partially integrated width is experimentally determined, which mixes both vector and axial(vector) in a non-trivial way. In [6] this limit has been used with a $|V_{ub}|$ value extracted over the full range of q^2 assuming Standard Model (SM). This explains the differences in the ϵ_R dependence in comparison to our Fig. 1 and their conclusion. The experimental $|V_{ub}|$ measurements do not need to be corrected for the ρ lineshape, as initially suggested in [7]

Details about the used experimental measurements can be found in [8]. The result of the χ^2 fit for $|V_{ub}^L| - \epsilon_R$ without and with the $B \to \rho\, \ell\bar{\nu}$ measurement are shown in Fig. 1.

The results presented here base on the work [8]. In Section 2 we derive the possible observables and discuss the form factors and their theoretical uncertainties in Section 3. The numerical predictions for the observables are presented in Section 4 and these are included for a global fit in the $|V_{ub}^L| - \epsilon_R$ plane in Sect. 5.

2. Possible Observables

For obtaining maximal information about the parameter ϵ_R, we derive the fully differential four body decay rate for the decay $B \to \rho[\to \pi\pi]\ell\bar{\nu}$. In order to describe the right-handed admixture given by the Lagrangian in Eq. (1), we need to replace in the matrix element the vector (V) and the three axial-vector ($A_{0,1,2}$) form factors via

$$V \to (1 + \epsilon_R)\, V, \qquad A_i \to (1 - \epsilon_R)\, A_i. \qquad (2)$$

With the additional assumption $\mathrm{Im}\, \epsilon_R = 0$ it can be done directly in the decay rate. In this talk we focus only on this case, further information on complex ϵ_R can be found in the corresponding article [8].

The decay rate can be written in terms of four variables. Conventionally we choose three angles, which describe the relative orientation of the final state particles. θ_V is the angle of the π^+ in the ρ restframe with respect to the ρ direction in the B restframe. Similarly, θ_ℓ is the angle of the ℓ^- in the dilepton restframe with respect to the direction of the virtual W^- in the B restframe. Finally χ is the angle between the decay planes of the hadronic and leptonic systems in the B restframe. Additionally we have the momentum transfer q^2 to the lepton system, while the invariant mass of the hadronic system is fixed by examine the on-shell decay, only. The fully differential rate, where the on-shell ρ meson is a pure P-wave, for massless leptons is written as

$$\frac{d\Gamma}{dq^2\, d\cos\theta_V\, d\cos\theta_\ell\, d\chi} = \frac{G_F^2 |V_{ub}^L|^2 m_B^3}{2\pi^4}$$
$$\times \Big\{ J_{1s} \sin^2\theta_V + J_{1c} \cos^2\theta_V$$
$$+ (J_{2s} \sin^2\theta_V + J_{2c} \cos^2\theta_V) \cos 2\theta_\ell$$
$$+ J_3 \sin^2\theta_V \sin^2\theta_\ell \cos 2\chi$$
$$+ J_4 \sin 2\theta_V \sin 2\theta_\ell \cos\chi + J_5 \sin 2\theta_V \sin\theta_\ell \cos\chi$$
$$+ J_{6s} \sin^2\theta_V \cos\theta_\ell + J_7 \sin 2\theta_V \sin\theta_\ell \sin\chi$$
$$+ J_8 \sin 2\theta_V \sin 2\theta_\ell \sin\chi + J_9 \sin^2\theta_V \sin^2\theta_\ell \sin 2\chi \Big\}. \qquad (3)$$

Our convention for the ranges of the angular variables are $\chi \in [0, 2\pi]$, $\theta_\ell \in [0, \pi]$, $\theta_V \in [0, \pi]$.

A fully differential analysis in four-dimensions in order to determine the J_i in bins of q^2 is experimentally challenging. In the following we propose to use observables in one, two and all three angles simultaneously. As we have shown in [8], these amount to simple counting experiments in different regions of phase space. All

of these observables are constructed such that the dependence on $|V_{ub}|$ drops out. To improve the statistical precision, we integrate over a suitably chosen interval of q^2. Given the available constraints on the form factors, we integrate over $0 \le q^2 \le 12\,\mathrm{GeV}^2$ to balance between experimental and theoretical uncertainties.

As we will see, it is important to estimate a reliable theoretical uncertainty for these observables. Especially the considered q^2 region is sizable, and hence we need to treat the uncertainties reliably in ratios of binned quantities. We develop a model for the uncertainties and correlations among the binned rates, using available calculations of the form factors.

2.1. One- dimensional asymmetries

The forward-backward asymmetry of the charged lepton is sensitive to the chiral structure of currents contributing to a decay,

$$A_{\mathrm{FB}} = \frac{\int_{-1}^{0} d\cos\theta_\ell (d\Gamma/d\cos\theta_\ell) - \int_{0}^{1} d\cos\theta_\ell (d\Gamma/d\cos\theta_\ell)}{\int_{-1}^{1} d\cos\theta_\ell \, (d\Gamma/d\cos\theta_\ell)}.$$
$$(4)$$

We study the sensitivity of this variable to ϵ_R in Sec. 4, after discussing the form factor inputs used. The one-dimensional distributions in χ and θ_V are symmetric, and hence it is not possible to construct asymmetry-type observables with good sensitivity to ϵ_R from these one-dimensional distributions.

2.2. Generalized Two- dimensional asymmetries

We found that if one integrates over one of the angles and defines two distinct regions in the remaining two angles, then integrating over χ results in the best sensitivity. To optimize the sensitivity from this class of measurements, we introduce new observables,

$$S = \frac{A - B}{A + B},$$
$$(5)$$

where A and B are the decay rates in two regions in the $\{\cos\theta_\ell, \cos\theta_V\}$ parameter space, chosen such that $S \simeq 0$ in the SM. This is a generalization of the forward-backward asymmetry, which may have increased sensitivity to ϵ_R. The optimal separation which discriminates between the two regions, A and B, depends on this choice of the q^2 range. Thus it is crucial to test the sensitivity of the result to nonperturbative uncertainties.

2.3. Three-dimensional Asymmetries

The previous approaches have the limitations of not allowing to chose the numerator and denominator arbitrarily in terms of the J_i functions, the extraction of the

full set of these coefficients is experimentally challenging. By allowing multiple regions in fairly large, $\pi/2$ size bins , we can extract each individual J_i by considering generalized asymmetries in multiple regions of all three angles. This method has been developed in [8]

$$J_i = \frac{1}{N_i} \sum_{j=1}^{8} \sum_{k,l=1}^{4} \eta_{i,j}^{\chi} \eta_{i,k}^{\theta_\ell} \eta_{i,l}^{\theta_V} \left[\chi^{(j)} \otimes \theta_\ell^{(j)} \otimes \theta_V^{(k)} \right].$$
$$(6)$$

Since some bin-boundaries need to be at half-integer multiples of $\pi/2$, we use a notation where $\chi^{(j)}$, $\theta_\ell^{(j)}$ and $\theta_V^{(k)}$ denote the 8 and 4 equal bins of size $\pi/4$, respectively. The corresponding normalization factors N_i and weighting factors $\eta_{i,j}^{\chi,\theta}$ can be found in [8]. Using this, we investigate the sensitivity of arbitrary ratios of the J_i in the following. This can be used for the extraction of observables in $B \to K^* \ell\ell$ in the same way, and in analogy with Ref. [15, 16, 17], we define

$$\langle P_1 \rangle_{\mathrm{bin}} = \frac{1}{2} \frac{\int_{\Delta q^2} dq^2 J_3}{\int_{\Delta q^2} dq^2 J_{2s}},$$
$$(7)$$

$$\langle P_5' \rangle_{\mathrm{bin}} = \frac{1}{2} \frac{\int_{\Delta q^2} dq^2 J_5}{\sqrt{-\int_{\Delta q^2} dq^2 J_{2s} \int_{\Delta q^2} dq^2 J_{2c}}},$$
$$(8)$$

which are, taking into account theoretical uncertainties, the most sensitive observables to a possible right-handed current. Furthermore, we find that we get best sensitivity for simple ratios, defined as

$$\langle P_{i,j} \rangle_{\mathrm{bin}} = \frac{\int_{\Delta q^2} dq^2 J_i}{\int_{\Delta q^2} dq^2 J_j}.$$
$$(9)$$

In particular, coefficients which depend on all three angles have good sensitivities, $\langle P_{3,4} \rangle$, $\langle P_{3,5} \rangle$, and $\langle P_{5,4} \rangle$.

3. Form Factor Fit

We use a series expansion, also known as the z expansion, to describe the form factor shape over the full range of the dilepton invariant mass [18]. In this paper we expand the form factors directly, instead of the helicity amplitudes. The series expansion uses unitarity to constrain the shape of the form factors, and implies a simple and well-motivated analytic parameterization over the full range of q^2. Defining $q_{\pm}^2 = (m_B \pm m_\rho)^2$, the form factors are written as

$$V(q^2) = \frac{1}{B_V(q^2) \, \Phi_V(q^2)} \sum_{k=0}^{K} \alpha_k^V z(q^2, q_0^2)^k,$$

$$A_i(q^2) = \frac{1}{B_{A_i}(q^2) \, \Phi_{A_i}(q^2)} \sum_{k=0}^{K} \alpha_k^{A_i} z(q^2, q_0^2)^k,$$
$$(10)$$

and the real q^2 axis is mapped onto the unit circle

$$z(q^2, q_0^2) = \frac{\sqrt{q_+^2 - q^2} - \sqrt{q_+^2 - q_0^2}}{\sqrt{q_+^2 - q^2} + \sqrt{q_+^2 - q_0^2}}. \quad (11)$$

The free parameter q_0^2 is chosen as $q_0^2 = (m_B + m_\rho)(\sqrt{m_B} - \sqrt{m_\rho})^2$, so that for the physical q^2 range of $B \to \rho\ell\bar{\nu}$ decay the expansion parameter is minimal, $|z(q^2, q_0^2)| \lesssim 0.1$. The so-called Blaschke factors in Eq. (10) for each form factor are $B_F(q^2) \equiv \prod_{R_F} z(q^2, m_{R_F}^2)$, where R_F are the sub-threshold resonances ($q_-^2 < m_{R_F}^2 < q_+^2$) with the quantum numbers appropriate for each form factor. By construction, $B_F(m_{R_F}^2) = 0$ and $|B_F(q^2)| = 1$ for $q^2 > q_+^2$. The main shape information is given by the functions [18]

$$\Phi_F(q^2) = \sqrt{\frac{1}{32\pi\chi_F(n)}} \frac{q^2 - q_+^2}{(q_+^2 - q_0^2)^{1/4}} \left[\frac{z(q^2, 0)}{-q^2}\right]^{(n+3)/2}$$
$$\times \left[\frac{z(q^2, q_0^2)}{q_0^2 - q^2}\right]^{-1/2} \left[\frac{z(q^2, q_-^2)}{q_-^2 - q^2}\right]^{-3/4}. \quad (12)$$

The only form factor dependent quantity is $\chi_F(n)$, which is related to the polarization tensor $\Pi_{\mu\nu}(q^2)$ at $q^2 = 0$, and n is the number of derivatives (subtractions) necessary to render the dispersion relation finite. This function is calculable in an operator product expansion. For the longitudinal part, involving A_0, one subtraction is necessary, while for the transverse part of the vector and axialvector current, involving the form factors A_1, A_2, and V, two subtractions are needed [18].

3.1. Correlation assumptions for the form factors

Unfortunately correlation information are currently not available from either lattice QCD or model calculations. We estimate these correlations in the light-cone QCD sum rule (LCSR) results [11, 19]. We distinguish two different kinds of correlations, (i) correlations among the different form factors at the same value of q^2; and (ii) correlations between different values of q^2, for the same form factors.

In Ref. [11], the uncertainties at $q^2 = 0$ are grouped into four sources, presumed uncorrelated: Δ_{7P}, Δ_{m_b}, Δ_L, and Δ_T. The values evaluated for $q^2 = 0$ are used in the following as an estimate of the uncertainties over a larger range of q^2. We investigate the individual contributions to these uncertainties and estimate the correlation among the form factors.

From these considerations, we can assess the correlated uncertainties in each contribution. In the following a model is tested to predict the correlations between

the form factors. For this model, according to the list above, the correlations between the A_i, and between the A_i and V are assumed to be $\{\rho_{7P}^{A_i}, \rho_{m_b}^{A_i}, \rho_L^{A_i}, \rho_T^{A_i}\} = \{\rho_{7P}^{V,A_i}, \rho_{m_b}^{V,A_i}, \rho_L^{V,A_i}, \rho_T^{V,A_i}\} = \{0.6, 1.0, 1.0, 1.0\}$. A full calculation of the form factors and the complete determination of the correlations is beyond the scope of this paper. Hence our estimate relies on the results given in that paper, and on our assumptions. This results in the correlation matrix for $\{V, A_0, A_1, A_2\}$ given by

$$C = \begin{pmatrix} 1. & 0.65 & 0.71 & 0.72 \\ 0.65 & 1. & 0.64 & 0.62 \\ 0.71 & 0.64 & 1. & 0.72 \\ 0.72 & 0.62 & 0.72 & 1. \end{pmatrix}. \quad (13)$$

This estimate is derived at $q^2 = 0$, and we use it for $q^2 > 0$ as well. Because of the constraints on the shapes of the form factors, no large change is expected far from maximal q^2.

The form factors at different values of q^2 are obtained from the same sum rule, however, the various contributions are weighted differently by q^2. For values of q^2 farther from one another, the correlation should decrease. Using the leading order results of [11], we found that the correlation for different values of q^2 only mildly depends on the separation, which we use below. Thus, uncertainties of a given form factor, A_i or V, for different q^2 are estimated to be 80% correlated, and we use a 1 GeV^2 binning in our analysis).

3.2. The χ^2 fit for the SE parameters

A simultaneous χ^2 fit to all sum rule points of Ref. [11] assuming the discussed correlations is performed. We verified the central values and uncertainties of the fit with ensembles of pseudo-experiments. The fit results can be found in [8].

The LCSR calculation result of the form factors is valid only for small q^2. However, the form factor shape changes by less than 1% when fitted in the region $q^2 < 7\,\text{GeV}^2$ or $q^2 < 14\,\text{GeV}^2$ [11]. Since the measurements in Ref. [10] are in 4 GeV bins, we restrict ourselves to fitting the data in the range $q^2 < 12\,\text{GeV}^2$ to balance between statistical sensitivity and theoretical validity.

4. Numerical Predictions of the Observables

In the following the theoretical predictions using the form factor input and uncertainties from the last section are discussed. The achievable sensitivity of the observables is estimated for 1 ab^{-1} and 50 ab^{-1} of integrated luminosity, corresponding to the available BABAR and Belle data sets and the anticipated Belle II data. The

treatment of their expected systematic and statistical uncertainty for the Neyman belt construction is explained in [8]. Experimental and theoretical uncertainties are assumed to be independent, and addition in quadrature is used to combine them. The sensitivity to a possible right-handed admixture is assessed by the interception of the uncertainty bands with the predicted SM value. In practice, every experiment will have to properly take into account all uncertainties for each value of ϵ_R.

4.1. Forward-backward asymmetry and the two-dimensional asymmetry, S

The prediction of A_{FB} including uncertainty estimates are shown in the left panel of Fig. 2. The central value is indicated by dotted lines and the blue band shows the theory uncertainty, as derived in the previous section. The red and green band show the total uncertainties for $1\,\text{ab}^{-1}$ and $50\,\text{ab}^{-1}$ of integrated luminosity, and the dashed vertical lines show the expected sensitivities assuming the SM. The theoretical and experimental uncertainties for $1\,\text{ab}^{-1}$ integrated luminosity are expected to be of similar size. For $50\,\text{ab}^{-1}$ integrated luminosity the dominant uncertainty will come from the $B \to \rho$ form factor.

The generalized two-dimensional asymmetry, S, requires to find a non-trivial dividing curve to define two distinct regions. The optimal contour in terms of sensitivity to right-handed admixtures is devised in [8]. The resulting curve most sensitive for ϵ_R, separating regions A and B, can be numerically approximated by

$$\cos\theta_V = \pm\sqrt{\frac{0.8472\cos^2\theta_\ell + 1.9038\cos\theta_\ell + 0.8472}{-1.1484\cos^2\theta_\ell + 1.9038\cos\theta_\ell + 2.8429}}.$$
(14)

This choice depends on nonperturbative input quantities as well as the considered q^2 interval.

The Neyman belt of S and sensitivities are shown in Fig. 2, the theoretical uncertainties are larger than for A_{FB}. The overall sensitivity on NP for $1\,\text{ab}^{-1}$ of integrated luminosity, however, is better due to the increased dependence on ϵ_R, and for $50\,\text{ab}^{-1}$ of data the sensitivity is comparable.

4.2. Simple generalized ratios

We have given a set of simple generalized observables, P_i, in Eq. (7-9), from which one expects the best theoretical sensitivity. The most sensitive observables in the context of real right-handed currents, are $\langle P_1 \rangle$, $\langle P_5' \rangle$ and $\langle P_{5,4} \rangle$. The corresponding predictions and sensitivities are shown in Fig. 3. The statistical correlations between the numerator and denominator in the

observables was estimated using Monte Carlo methods, neglecting any influence from background. The three-dimensional observables reduce the theoretical uncertainties with respect to the one-dimensional or two-dimensional asymmetries. Their experimental uncertainties, however, are larger due to the great number of free parameters that need to be determined from the same data. The most precise observable for $1\,\text{ab}^{-1}$ of integrated luminosity is $\langle P_{5,4} \rangle$.

5. Global Fit

The estimated sensitivities on ϵ_R in the previous section can be used to add an orthogonal constraint to the global fit performed in Section 1. The gain in overall sensitivity on $|V_{ub}^L|$ and ϵ_R is estimated by extrapolating the experimental uncertainties to $1\,\text{ab}^{-1}$ and $50\,\text{ab}^{-1}$.

Fig. 4 shows the results for the simultaneous fit for $|V_{ub}^L|$ and ϵ_R for integrated luminosities of $1\,\text{ab}^{-1}$ and $50\,\text{ab}^{-1}$. The fits incorporate the expected constraints from either A_{FB}, S, or $P_{5,4}'$ in the absence of right-handed currents. For the $1\,\text{ab}^{-1}$ scenario, the current experimental central values are used for $|V_{ub}|$, whereas for $50\,\text{ab}^{-1}$ the SM is assumed, with identical $|V_{ub}|$ from all channels. For $1\,\text{ab}^{-1}$ B-factory data, S results in the largest gain in sensitivity for right-handed currents among the studied observables. Table 2 lists the reduction of the uncertainty of $|V_{ub}^L|$ and ϵ_R with respect to a fit without any additional orthogonal bound. Although the theoretical uncertainties on S are more sizable than on $P_{5,4}'$, the experimental simplicity of the two-dimensional asymmetry results in the best overall expected sensitivity. The reduction in experimental uncertainties for $50\,\text{ab}^{-1}$ statistics changes this picture: here the theoretical uncertainties on the $B \to \rho$ form factors dominate the overall uncertainty of all observables and $P_{5,4}'$ results in the best expected sensitivity.

Fit	$\delta\left(\left|V_{ub}^L\right|\right)$ [%]	$\delta\left(\epsilon_R\right)$ [%]
4 modes + A_{FB} ($1\,\text{ab}^{-1}$)	-0.3	-5
4 modes + S ($1\,\text{ab}^{-1}$)	-0.5	-9
4 modes + $P_{5,4}$ ($1\,\text{ab}^{-1}$)	-0.5	-8
4 modes + A_{FB} ($50\,\text{ab}^{-1}$)	-0.4	-2
4 modes + S ($50\,\text{ab}^{-1}$)	-0.5	-2
4 modes + $P_{5,4}$ ($50\,\text{ab}^{-1}$)	-3	-10

Table 2: The expected relative reduction in the uncertainty of $\left|V_{ub}^L\right|$ and ϵ_R for the χ^2 fits in Figs. 4. The improvements are quoted with respect to the expected uncertainties on the 4-mode analysis for $1\,\text{ab}^{-1}$ and $50\,\text{ab}^{-1}$, which are $\Delta\left(\left|V_{ub}^L\right| \times 10^3, \Delta\epsilon_R\right) = (0.18, 0.061)$ and $(0.06, 0.016)$, respectively.
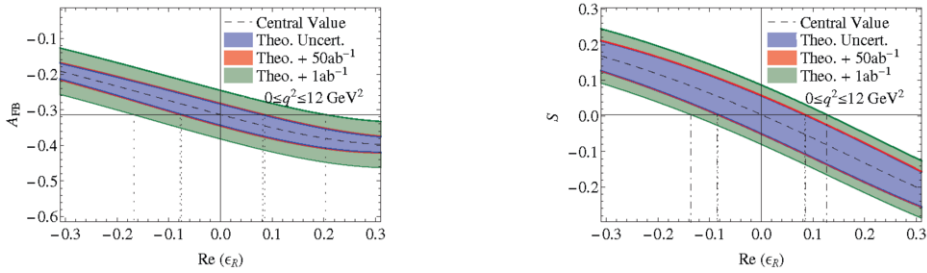
Figure 2: Predictions for the forward-backward asymmetry (left) and S (right), including theoretical uncertainties (blue band), and theory and experimental uncertainties combined in quadrature for $50\,\mathrm{ab}^{-1}$ (orange) and $1\,\mathrm{ab}^{-1}$ (green).
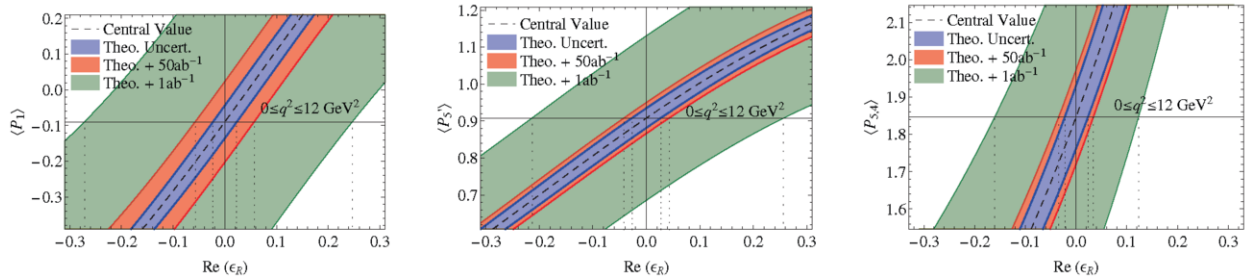

Figure 3: The most sensitive angular observables to Re ϵ_R. The blue bands show the theoretical uncertainties, while the orange [dark-green] bands show theory and experimental uncertainties combined in quadrature, for $50\,\mathrm{ab}^{-1}$ [$1\,\mathrm{ab}^{-1}$] of B-factory data. The observables, $\langle P_1 \rangle$ (left), $\langle P_5' \rangle$ (center), $\langle P_{5,4} \rangle$ (right), are defined in Eqs. (7)–(9).

6. Discussion and Conclusions

In this talk, the full decay distribution in semileptonic $B \to \rho[\to \pi\pi]\ell\bar{\nu}$ decay was analyzed to explore the consequences of a possible right-handed semileptonic current from physics beyond the Standard Model. A number of observables was explored, some new and some defined in the literature. We performed a detailed investigation of the impact of the theoretical uncertainties, using a model for the correlations, on the sensitivity.

To set a bound on this beyond Standard Model contribution, two approaches are possible: (i) a full four-dimensional fit for the J_i coefficients or counting experiments that involve determining the partial branching fraction in several regions of phase space and combining this information appropriately to project out either the J_i coefficients, or (ii) to construct asymmetries sensitive to NP contributions in two distinct phase-space regions. The latter offer an obvious alternative, since with the currently available B-factory data, a full four-dimensional fit appears to be a very challenging endeavor.

The discussed observables exhibit very different theoretical and experimental uncertainties: besides the usual forward-backward asymmetry, a two-dimensional generalized asymmetry is proposed by integrating out one

of the decay angles form the fully differential decay rate. These two are experimentally the simplest observables. A set of generalized three-dimensional observables is discussed. These are experimentally more challenging, and the eventual observables involve ratios of statistically and systematically correlated observables.

A ranking in terms of sensitivity reveals that the balance of experimental and theoretical uncertainties is important: for the available B-factory statistics of about $1\,\mathrm{ab}^{-1}$, the two dimensional asymmetry S with its simple experimental definition seems to be the most sensitive to the presence of right-handed currents. For the anticipated $50\,\mathrm{ab}^{-1}$ Belle II statistics, the more complicated three-dimensional observables result in the best expected sensitivity due to the reduction of experimental uncertainties. A direct determination of ϵ_R allows to introduce an orthogonal constraint into the indirect determination involving $|V_{ub}|$ measurements from various decays with different ϵ_R dependencies. Including the most sensitive direct ϵ_R constraint for $1\,\mathrm{ab}^{-1}$ or $50\,\mathrm{ab}^{-1}$, reduces the uncertainty of ϵ_R by about 10% in such a global analysis. This implies that even with the current B-factory datasets a useful statement about ϵ_R from $B \to \rho\ell\nu$ can be obtained.

ST thanks the organizers of ICHEP 2014 for hosting the conference and giving me the opportunity to

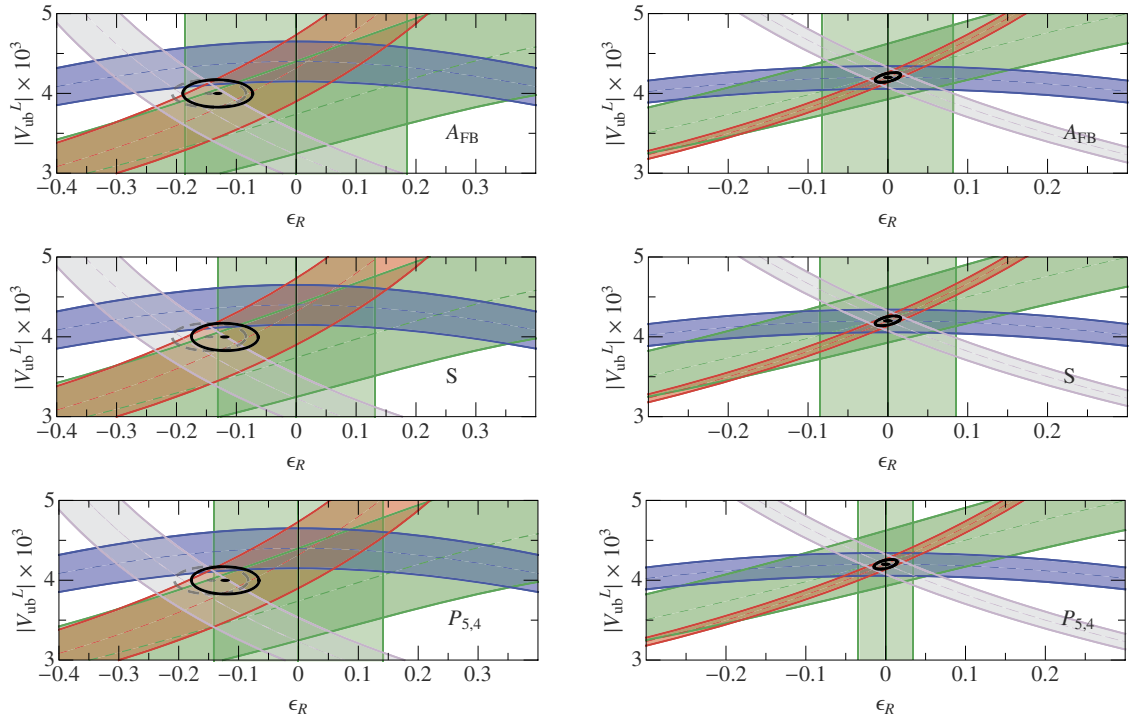Figure 4: The χ^2 fits for $|V_{ub}^L|$ and ϵ_R assuming 1 ab^{-1} (left) and 50 ab^{-1} (right) of B-factory data. The green bands show the $B \to \rho\ell\bar{\nu}$ information, c.f., Fig. 1. The observable used for the expected orthogonal bound on ϵ_R, assuming the SM, is shown in each Figure. Table 2 lists the improvement in uncertainty by including the orthogonal constraint from the discussed observable on ϵ_R with respect to the uncertainty of fitting the experimental information available by $B \to X_u\ell\bar{\nu}$, $B \to \tau\bar{\nu}$, $B \to \pi\ell\bar{\nu}$, and $B \to \rho\ell\bar{\nu}$ only.

References

[1] J. Charles, S. Descotes-Genon, Z. Ligeti, S. Monteil, M. Papucci and K. Trabelsi, Phys. Rev. D **89**, 033016 (2014) [arXiv:1309.2293 [hep-ph]].

[2] C. H. Chen and S. h. Nam, Phys. Lett. B **666** (2008) 462 [arXiv:0807.0896 [hep-ph]].

[3] A. Crivellin, Phys. Rev. D **81**, 031301 (2010) [arXiv:0907.2461 [hep-ph]].

[4] A. J. Buras, K. Gemmler and G. Isidori, Nucl. Phys. B **843**, 107 (2011) [arXiv:1007.1993 [hep-ph]].

[5] S. Faller, T. Mannel and S. Turczyk, Phys. Rev. D **84** (2011) 014022 [arXiv:1105.3679 [hep-ph]].

[6] A. Crivellin and S. Pokorski, arXiv:1407.1320 [hep-ph].

[7] X. W. Kang, B. Kubis, C. Hanhart and U. G. Meiner, Phys. Rev. D **89** (2014) 053015 [arXiv:1312.1193 [hep-ph]].

[8] F. U. Bernlochner, Z. Ligeti and S. Turczyk, arXiv:1408.2516 [hep-ph].

[9] Y. Amhis *et al.* [Heavy Flavor Averaging Group], arXiv:1207.1158 [hep-ex]; and updates at http://www.slac.stanford.edu/xorg/hfag/.

[10] A. Sibidanov *et al.* [Belle Collaboration], Phys. Rev. D **88**, 032005 (2013) [arXiv:1306.2781 [hep-ex]];

[11] P. Ball and R. Zwicky, Phys. Rev. D **71**, 014029 (2005) [hep-ph/0412079].

[12] S. W. Bosch, B. O. Lange, M. Neubert and G. Paz, Nucl. Phys. B **699** (2004) 335 [hep-ph/0402094].

[13] B. Aubert *et al.* [BaBar Collaboration], Phys. Rev. D **77**, 032002 (2008) [arXiv:0705.4008 [hep-ex]].

[14] W. Dungel *et al.* [Belle Collaboration], Phys. Rev. D **82**, 112007 (2010) [arXiv:1010.5620 [hep-ex]].

[15] J. Matias, F. Mescia, M. Ramon and J. Virto, JHEP **1204**, 104 (2012) [arXiv:1202.4266 [hep-ph]].

[16] S. Descotes-Genon, T. Hurth, J. Matias and J. Virto, JHEP **1305** (2013) 137 [arXiv:1303.5794 [hep-ph]].

[17] S. Descotes-Genon, J. Matias, M. Ramon and J. Virto, JHEP **1301** (2013) 048 [arXiv:1207.2753 [hep-ph]].

[18] A. Bharucha, T. Feldmann and M. Wick, JHEP **1009** (2010) 090 [arXiv:1004.3249 [hep-ph]].

[19] C. Hambrock, G. Hiller, S. Schacht and R. Zwicky, arXiv:1308.4379 [hep-ph].